ADVANCED FUNCTIONAL MATERIALS
www.afm-journal.de

www.MaterialsViews.com

The Criteria for Beneficial Disorder in Thermoelectric Solid Solutions

Heng Wang, Aaron D. LaLonde, Yanzhong Pei, and G. Jeffery Snyder**

Forming solid solutions has long been considered an effective approach for good thermoelectrics because the lattice thermal conductivities are lower than those of the constituent compounds due to phonon scattering from disordered atoms. However, this effect could also be compensated by a reduction in carrier mobility due to electron scattering from the same disorder. Using a detailed study of n-type $(PbTe)_{1-x}$ $(PbSe)_x$ solid solution ($0 \le x \le 1$) as a function of composition, temperature, and doping level, quantitative modeling of transport properties reveals the important parameters characterizing these effects. Based on this analysis, a general criterion for the improvement of zT due to atomic disorder in solid solutions is derived and can be applied to several thermoelectric solid solutions, allowing a convenient prediction of whether better thermoelectric performance could be achieved in a given solid solution. Alloying is shown to be most effective at low temperatures and in materials that are unfavorable for thermoelectrics in their unalloyed forms: high lattice thermal conductivity (stiff materials with low Grüneisen parameters) and high deformation potential.

1. Introduction

Energy recovery from waste heat at elevated temperatures is attracting interest due to the increased demand of higher fuel efficiency and smaller environmental impact. Thermoelectric generation enables the direct heat to electricity conversion thus is desirable for such applications.[1] Developing bulk materials with high figure of merit, zT, defined as $zT = S^2\sigma T/(\kappa_e + \kappa_L)$ (S is the Seebeck coefficient, σ is the electric conductivity, and κ_e and κ_L are the electronic and lattice thermal conductivity, respectively), is the focus of thermoelectric materials research.[2,3] PbTe and its alloys are widely studied for applications around 500–900 K. Various efforts have been made to achieve higher zT at this temperature range via nanostructuring[3,4] and energy band distortion.[5] Studies have also shown that when doped properly high quality PbTe would demonstrate its inherent maximum zT of 1.5 (p-type[6]) and 1.4 (n-type[7]). On the other hand PbSe, the analog of PbTe containing much cheaper element of Se was also found to have maximum zT of 1.2 in both p type[8] and n type materials.[9,10]

Further improving of zT should be through material engineering to produce more favorable features over conventional materials.[11] A good example is by forming solid solutions[12] (i.e. alloying), which has been successfully used in systems such as $Si_{1-x}Ge_x$,[13] $Mg_2Si_{1-x}Sn_x$,[14] $Bi_{2-x}Sb_xTe_3$ (or $Bi_2Te_{3-x}Se_x$)[15,16] and half-Heusler compounds (for instance[17] $Hf_{1-x}Zr_xNiSn_{1-y}Sb_y$). The alloying of IV–VI compounds has also been studied in history for their influence on thermal, electrical and mechanical properties. Results are reported by for instance Ioffe,[18] Stil'bans,[16,19] and Alekseeva.[20] Recent incorporation of alloying with the concept of energy band engineering has enabled zT improvement in p type $PbTe_{1-x}Se_x$,[11,21] $Pb_{1-x}Cd_xTe$[22] and $Pb_{1-x}Mg_xTe$.[23] As the band structure engineering approach does not explicitly involve additional phonon and electron scattering, its effect should be characterized separately and is not included in following analysis of phonon and electron scattering from the atomic disorder.

In solid solutions, defects from atomic disorder act as scattering centers for phonons leading to the lattice thermal conductivity reduction. At the same time this disorder causes local potential energy fluctuations that induces additional charge carrier scattering resulting in mobility reduction as well. In thermoelectric material research, these effects are often considered qualitatively, sometimes even one-sided. There are, however quantitative transport models that could weigh the magnitude of each reduction. For example the model developed by Callaway[24] and Klemens[25] for thermal conductivity in solid solutions due to point defect scattering have been widely used in various materials systems.[11,26,27] On the other side the electronic transport perturbed by atomic disorder was also studied since the 1930s by Nordheim[28] in metal alloys and later Brooks[29] and Glicksman[30] in Si-Ge.

The thermoelectric quality factor B used by Chasmar and Stratton[31] determines the optimized zT of thermoelectrics when the dominant scattering mechanism is known. For materials used above room temperature with the absence of bipolar effects the charge carrier scattering is dominated by phonons through non-polar processes, then according to deformation potential scattering theory:[32]

H. Wang, Dr. A. D. LaLonde, Dr. Y. Pei,[+] Prof. G. J. Snyder
Materials Science, California Institute of Technology
Pasadena, CA 91125, USA
E-mail: peiyanzhong@gmail.com; jsnyder@caltech.edu
[+] Present address: School of Materials Science and Engineering, Tongji University, 4800 Caoan Road, Shanghai 201804, China

DOI: 10.1002/adfm.201201576

$$B = T\frac{2k_B^2\hbar}{3\pi}\frac{C_l N_V}{m_I^* \Xi^2 \kappa_L} \quad (1)$$

where C_l is the average longitudinal elastic constant,[33] N_v is the valley degeneracy of conducting band, m_I^* is the inertial effective mass and Ξ the effective deformation potential coefficient for non-polar phonon scattering. The quality factor B in Equation (1) accounts for a single type of electron scattering while for disordered crystals the additional alloy scattering should also be included.

Here we studied the n-type $(PbTe)_{1-x}(PbSe)_x$ solid solution throughout the composition range, which is an ideal system for the quantitative study of disorder in thermoelectrics. Well determined transport parameters of PbTe and PbSe are available in literature[34] and have been confirmed by our previous studies.[7,9] The two compounds are completely miscible throughout the composition range. The conduction band structure of both are very similar and simple showing single band behavior, which enables the discussion and understanding of transport properties using a relatively simple model, without involving the complexity of changing band structure when forming solid solutions. Our result demonstrated the validity of transport models commonly used in describing the additional phonon and electron scattering due to disorder. The key parameters derived from these models were further incorporated into B to obtain a comprehensive evaluation of their influence on material figure of merit. We have found that B and zT are unchanged throughout the solid solution composition in n-type $(PbTe)_{1-x}(PbSe)_x$. The analysis applied in this work is consolidated as general criteria to estimate the potential of zT improvement by introducing atomic disorder and these criteria are demonstrated in several thermoelectric solid solutions.

2. Results and Discussions

2.1. Band Structure and Seebeck Coefficient

The phase purity and the typical solid solution behavior were first checked by X-ray diffraction (XRD) on sintered samples. Single FCC phase was observed in all samples under XRD. Lattice parameters were extrapolated from high angle diffraction peaks and are found changing with composition as predicted by Vegard's law (the dashed line in **Figure 1**). The same trend has also been observed in previous study.[11] As Vegard's law is obeyed by all solid solutions with atomic level random distribution, all the samples are thus considered as solid solutions and the nano-scale compositional fluctuation is not explicitly considered.

The band structures of lead chalcogenides (PbTe, PbSe and PbS) are described with a model that features two bands on the valence band side.[34] Despite the band structure being suggested more complicated,[35] this model explains the transport properties very well.[6,11]

The conduction band of both PbTe and PbSe contains a single minimum at L point of the first Brillouin zone.[36] The dispersion relation near the band edge can be better approximated with the non-parabolic Kane band model,[7,37–39] instead

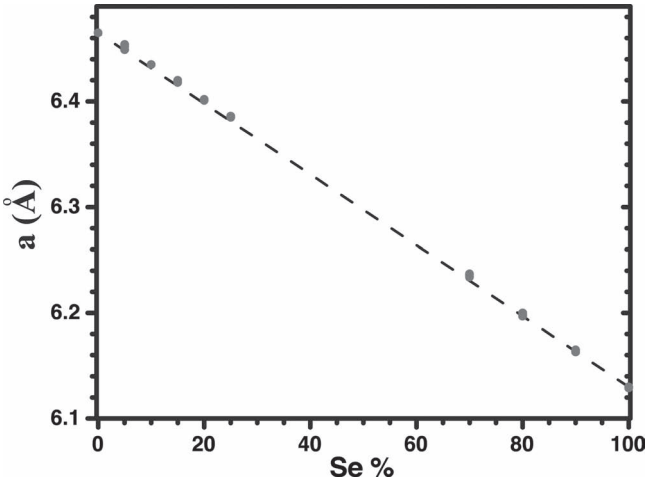

Figure 1. Lattice constants of $(PbTe)_{1-x}(PbSe)_x$ solid solutions as function of Se content, being consistent with Vegard's law.

of the parabolic band model. These basic band features should apply for the solid solution between them.

The difference in band structure affects the transport properties, which is understood primarily through the effective mass (when the minority carriers are negligible). The total density-of-state effective mass m_d^* are very similar[7,9,34] for the conduction band in PbTe and PbSe. This quantity for their solid solution is also found nearly independent of composition. To demonstrate this the Seebeck coefficients were plotted against Hall carrier density at different temperatures in **Figure 2**. The solid lines are calculated results using $m_{d,300K}^* = 0.27\ m_e$ and $dLnm_d^*/dLnT = 0.45$ (parameters taken from our previous study) under the acoustic phonon scattering dominant assumption and the single Kane band (SKB) model. The open symbols are from PbTe (squares) and PbSe (circles), both showing good agreement with the calculated curves. The Seebeck coefficients of solid solutions are also found following the same trend regardless of their composition. In other words m_d^* does not change in n type $(PbTe)_{1-x}(PbSe)_x$ and samples with

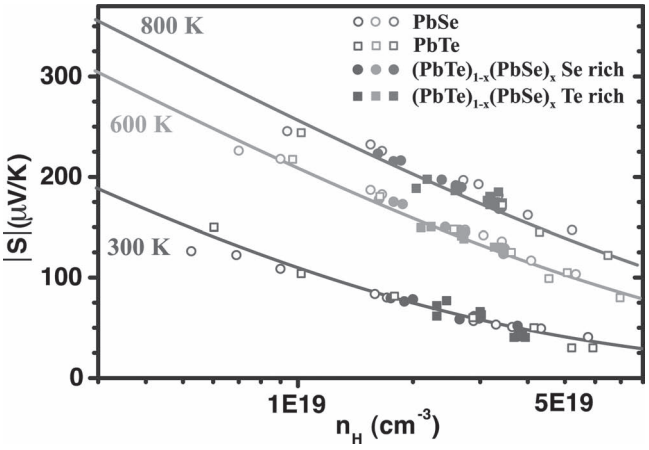

Figure 2. Seebeck coefficient versus Hall carrier density of $(PbTe)_{1-x}(PbSe)_x$ solid solutions at different temperatures, data for binary PbTe and PbSe are also shown.

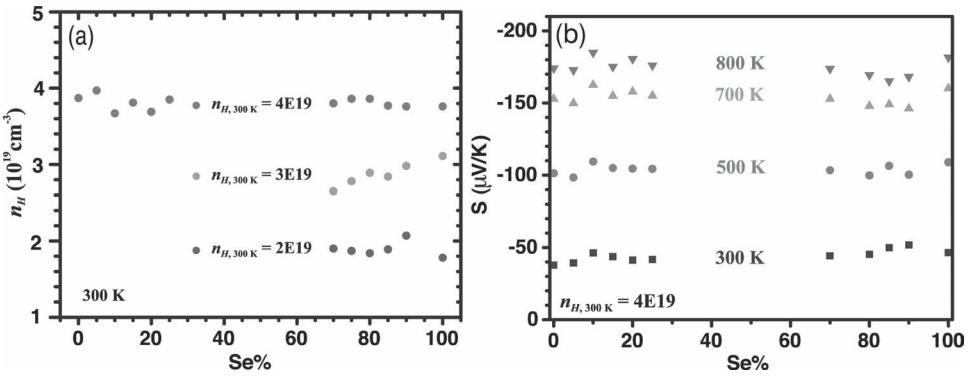

Figure 3. a) Hall carrier density (300 K) and b) Seebeck coefficient ($n_{H,\,300K}$ = 4E19) as function of alloy composition.

similar Hall carrier density would have similar Seebeck coefficient values.

Halogens do not change the band structure of lead chalcogenides.[34,40] The substitution of Br and I for Se and Te adds one electron per atom to the conduction band as long as these electrons are delocalized. Delocalization occurs at sufficiently high dopant concentrations and temperatures measured in this study. This allows the following discussion on the carrier concentration dependent Seebeck coefficient without involving additional band structure modification due to I- or Br-doping. **Figure 3** shows the Hall carrier density and Seebeck coefficient as function of alloy composition. It demonstrates the consistency of S values among samples with different composition but similar doping level. The very small fluctuation in n_H and S within each group, named after their nominal Hall carrier density at 300 K, assures that the following discussions are based on results not affected by carrier density (or chemical potential) difference.

The band gap of PbTe and PbSe are 0.19 eV and 0.17 eV (0 K), respectively.[41] Temperature dependence of $+4 \times 10^{-4}$ eVK^{-1} was determined[42] experimentally using optical methods for both compounds. According to the two-valence-band model, the band gaps saturate at 0.36 eV for PbTe and 0.47 eV for PbSe when the energy level of L valence band reaches that of the temperature independent Σ band. However how the band gap changes in $(PbTe)_{1-x}$ $(PbSe)_x$ solid solutions at high temperatures has not been studied and it is thus assumed that the band gaps of solid solutions are linear combinations of those of two binary compounds at that temperature. We note that the experimental results on optical band gap measurements is consistent with this assumption within 0.02 eV in undoped samples at both 77 K[43] and 300 K.[44] This is true even for doped samples[45] with influence from free carrier absorption.

2.2. Mobility Reduction Due to Alloy Scattering

In solid solutions an additional scattering mechanism of carriers is introduced due to the random distribution of different atoms on the same lattice site. The mobility of solid solution is thus lower than that of pure compound. In **Figure 4** the drift mobility ($\mu = \mu_H/A$, A is the Hall factor calculated as a function of the chemical potential which is further obtained from measured Seebeck coefficient, see ref. 8 supporting information for detail. For the doping range studied here A is found around 1.17 at room temperature) is plotted as function of alloy composition. The mobility drops dramatically as a small amount of substitutional atoms (x ~ 0.05) were introduced and then gradually saturate and reach a region after x > 0.3 where the mobility is relatively insensitive to alloy composition. Two sets of room

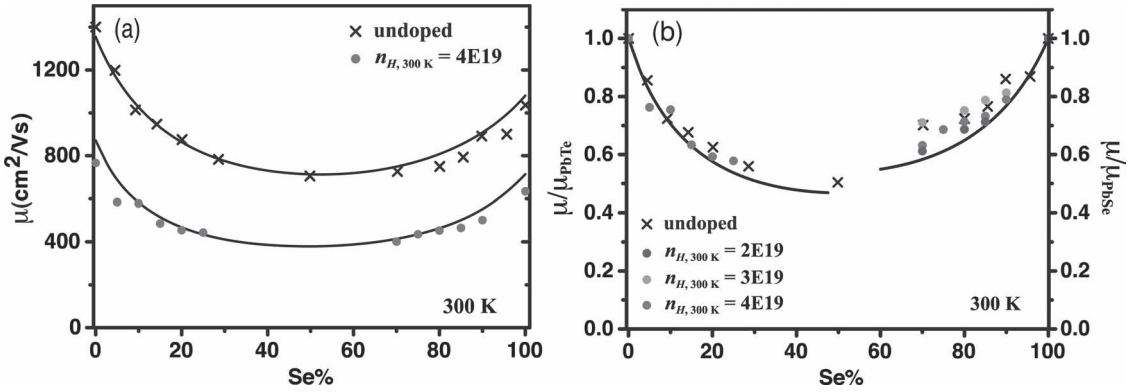

Figure 4. The drift mobility at 300 K for $(PbTe)_{1-x}(PbSe)_x$ solid solutions with different doping levels. a) drift mobility b) reduction relative to PbSe or PbTe. Solid lines are calculated results taking into account the alloy scattering of carriers.

temperature data are included in Figure 4a). The dots are from samples with carrier density of about 4×10^{19} cm^{-3}. The crosses are for undoped samples taken from Efimova and Stil'bans' report.[19]

The atomic level disorder in solid solution produces potential energy fluctuation, which is analogous to the deformation potential caused by phonon waves (which induces acoustic phonon scattering) and is usually called disorder scattering[46] or alloy scattering. Such effect was first studied by Nordheim[28] in metal alloys from the 1930s and the associated electron relaxation time τ_{alloy} was shown depending on alloy composition and carrier energy. Brooks[29] later pointed out that τ_{alloy} also has a temperature dependence of $T^{-1/2}$ as oppose to the $T^{-3/2}$ dependence for acoustic phonon scattering. Glicksman et al.[30,46a] studied Si-Ge and III–V alloys and developed the expression for mobility due to alloy scattering. The first explicit expression of relaxation time τ_{alloy} was later developed by Harrison and Hauser[46,47] for nondegenerate III–V semiconductors:

$$\tau_{0alloy} = \frac{8\hbar^4}{3\sqrt{2}\pi\,\Omega x(1-x)U^2 m_b^{*3/2}(k_B T)^{1/2}}\varepsilon^{-1/2} \tag{2}$$

Here Ω is the volume per atom, x is the concentration fraction of the alloying atom, U is the alloy scattering potential which determines the magnitude of the alloy scattering for the given alloy, m_b^* is the density-of-state effective mass for a single valley and ε is the reduced carrier energy $\varepsilon = E/k_BT$. Note that Equation (2) was derived for nondegenerate semiconductors under the single parabolic band assumption. Thus for the single Kane band model taking into account band nonparabolicity, arbitrary degeneracy and energy dependent electron phonon interaction[37] (being analogous to the relaxation time for acoustic phonon scattering), the equation above is generalized as:

$$\tau_{alloy} = \frac{8\hbar^4}{3\sqrt{2}\pi\,\Omega x(1-x)U^2 m_b^{*3/2}(k_B T)^{1/2}} \times (\varepsilon + \varepsilon^2\alpha)^{-1/2}(1+2\varepsilon\alpha)^{-1}\left[1-\frac{8\alpha(\varepsilon+\varepsilon^2\alpha)}{3(1+2\varepsilon\alpha)}\right]^{-1} \tag{3}$$

Here $\alpha = k_BT/\varepsilon_g$, ε_g being the gap between conduction band and valence band at L point.

The total relaxation time is given by Matthiessen's rule:

$$\tau_{total}^{-1} = \tau_{pure}^{-1} + \tau_{alloy}^{-1} \tag{4}$$

For the relaxation time without the alloy effect τ_{pure}, the nonpolar deformation potential (acoustic) phonon scattering is used (τ_{ac}):[9,34]

$$\tau_{ac} = \frac{\pi\hbar^4 C_l}{2^{1/2} m_b^{*3/2}(k_B T)^{3/2}\Xi^2} \times (\varepsilon + \varepsilon^2\alpha)^{-1/2}(1+2\varepsilon\alpha)^{-1}\left[1-\frac{8\alpha(\varepsilon+\varepsilon^2\alpha)}{3(1+2\varepsilon\alpha)}\right]^{-1} \tag{5}$$

Parameters in equation (5) have been determined in previous studies on n-type PbTe[7] and PbSe.[9] For a given alloy composition, τ_{ac} is assumed to be the linear combination of the two binary compounds. In lightly doped lead chalcogenides the polar scattering from optical phonons (with relaxation time τ_{po}) was also observed[38] therefore this mechanism is also considered.

$$\tau_{pure}^{-1} = \tau_{po}^{-1} + \tau_{ac}^{-1} \tag{6}$$

Once the total relaxation time is determined the mobility can be calculated from:[34]

$$\mu = \frac{e}{m_I^*}\frac{\int_0^\infty(-\frac{\partial f}{\partial\varepsilon})\tau_{total}(\varepsilon)(\varepsilon+\alpha\varepsilon^2)^{3/2}(1+2\alpha\varepsilon)^{-1}d\varepsilon}{\int_0^\infty(-\frac{\partial f}{\partial\varepsilon})(\varepsilon+\alpha\varepsilon^2)^{3/2}d\varepsilon} \tag{7}$$

The calculated results are plotted in Figure 4 as solid curves. Most parameters used in the modeling are supported by independent experimental measurements. The only undetermined parameter is the alloy scattering potential U, which is assumed temperature and composition independent. In this study U was found to be 1.1 eV for n type $(PbTe)_{1-x}(PbSe)_x$ system by fitting the experimental data in Figure 4a). With no other adjustable parameters this model explains quantitatively the observed mobilities at 300 K extremely well for samples with and without doping.

The alloy scattering relaxation time τ_{alloy} has the same energy and effective mass dependence as does acoustic phonon scattering τ_{ac}. This indicates that its relative importance to the acoustic phonon scattering is fixed at a given temperature and alloy composition regardless of the doping level. This is confirmed by our experiment (Figure 4 (b)) as the relative reduction of mobility described by μ/μ_{PbX}, where μ_{PbX} is the mobility of corresponding matrix compound with the same carrier density, is the same for sets of samples with different doping level.

As the temperature increases the current model tends to overestimate the mobilities. The same deviation was also observed in n type PbSe without disorder.[9] A good fit at 800 K could be made allowing the effective deformation potential coefficient Ξ to increase by 15% (**Figure 5**). Ξ is generally considered temperature independent and the apparent increase could have several different origins. For instance the influence from minority carriers at high temperature or the decrease of elastic constants (C_l) with temperature, both are not included in the current model so that the phenomenological adjustment of Ξ is used to accommodate their influence while keeping the simplicity of the model. It is also possible that the temperature activated deformation potential scattering from optical phonons[48] or inter-valley scattering[49] does make the effective deformation potential coefficient Ξ to slightly increase over a wide temperature range.

The value of alloy scattering potential U is of key importance to the magnitude of mobility reduction at a given composition. Values of U, however, are available only for a few systems.[50a–e] These are shown in **Table 1** along with some other physical property differences[46c,51a,b] of the alloy components. The typical magnitude of U is found between 0.6 to 2 eV, which is much smaller than a typical effective deformation potential coefficient Ξ (8 to 35 eV[9]). The value of U should be, according to Brooks,[29] related to the band gap difference. This is claimed[46c,52] later to be inaccurate to calculate U whereas the

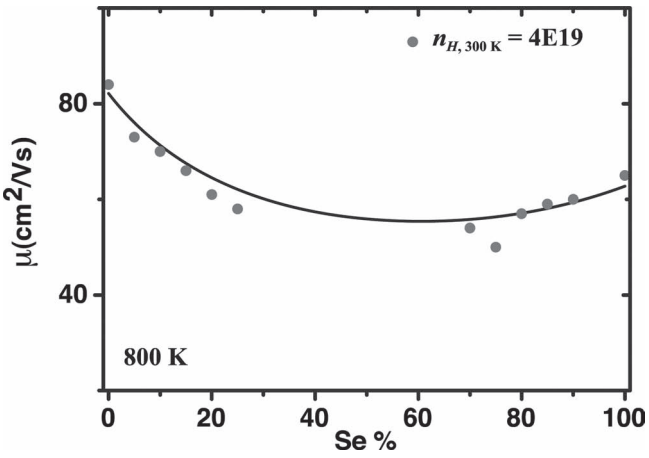

Figure 5. The drift mobility at 800 K for $(PbTe)_{1-x}(PbSe)_x$ solid solutions, samples are with similar Hall carrier density. The solid curve is calculated from the model described in the text.

difference of electron affinity might be a possible alternative. Neither of these could however explain the value of *U* found for n-type PbTe-PbSe, as both the band gap and electron affinity difference between PbTe and PbSe are very small.

2.3. Lattice Thermal Conductivity Reduction Due to Point Defect Scattering

Despite their lower mobility the solid solutions are still of great interest for thermoelectric applications because of another important effect of alloying: the reduction of lattice thermal conductivity. The effect of alloying on lattice thermal conductivity is accounted for by introducing the point defect scattering of phonons.

Table 1. A comparison of the alloy scattering potential *U* in a few solid solutions together with the difference between two constituents in electron affinity ΔX, band gap ΔE_g, molar mass ΔM, and lattice parameter $\Delta\alpha$. M_h, α_l stands for the heavier one and the larger one of the two compounds, respectively.

Alloy system	ΔX [eV]	ΔE_g [eV]	ΔM (ΔM/M_h)	$\Delta\alpha$ ($\Delta\alpha/\alpha_l$) [Å]	U [eV]	Note
n-$Al_{1-x}Ga_xN$	3.5[a]	2.69	42.7 (61%)	0.21 (4%)	1.5–2.0[b]	Δa compare c direction, U numerical calculation
n-$Al_{1-x}Ga_xAs$	0.43[a]	1.72	42.7 (61%)	0.01 (0.1%)	1.1[c]	U numerical calculation
n-$Cd_{1-x}Zn_xTe$	0.8[d,e]	0.88	88.2 (44%)	0.37 (6%)	1.1 (0.4)[f]	
n-$InAs_{1-x}P_x$	0.5[g]	0.99	44 (58%)	0.19 (3%)	0.6[h]	
n-$Si_{1-x}Ge_x$	0.05[a]	0.46	44.5 (60%)	0.23 (4%)	0.6 – 1.0[i]	
n-$PbSe_{1-x}Te_x$	0.1[j]	0.02	48.6 (38%)	0.33 (5%)	1.1	U from this work

Taken from [a]Ref. [62]; [b]Ref. [50a]; [c]Ref. [50b]; [d]Ref. [51a]; [e] Ref. [51b]; [f] Ref. [50c]; [g]Ref. [46c]; [h]Ref. [50d]; [i]Ref. [50e]; [j] Ref. [50f].

For high quality, pure compounds assuming Umklapp phonon scattering dominance, the thermal conductivity is:[53,54]

$$\kappa_L = C'\left(\frac{k_B}{h}\right)^3 \frac{\Omega^{1/3} M\theta_D^3}{\gamma^2 T} = C\frac{Mv^3}{T\Omega^{2/3}\gamma^2} \quad (8)$$

Here v is the averaged speed of sound, θ_D is the Debye temperature, M is the averaged atomic weight and γ the Grüneisen parameter. The factor C used by Toberer et al.[53] is $(6\pi^2)^{2/3}/4\pi^2$ while other values were also suggested by different researchers.[53,54] In lead chalcogenides such $1/T$ behavior was observed,[34] which implies the Umklapp process being dominant. Equation (8), when applied for PbTe and PbSe, overestimates the lattice thermal conductivity at 300 K by a factor of 2 (exact value is sensitive to the choice of Debye temperature). This is probably due to the recently discussed strong coupling between optical and acoustic phonons.[55]

If the scattering from interfaces is further negligible, as is the case for high quality materials without nano-structuring, the only existing phonon scattering mechanism in solid solutions would be the Umklapp scattering and the point defect scattering. The following relation between $\kappa_{L,alloy}$ and that of the pure compound $\kappa_{L,pure}$ is proposed by Callaway[24] and Klemens[25] in such framework and has been successfully used in various alloy systems:[11,26,56–58]

$$\frac{\kappa_{L,alloy}}{\kappa_{L,pure}} = \frac{arctan(u)}{u},\ u^2 = \frac{\pi\theta_D\Omega}{2\hbar v^2}\kappa_{L,pure}\Gamma \quad (9)$$

The scattering parameter Γ was studied in detail by Klemens[25,61] taking into account influences from mass difference, binding force difference and strain field induced by a point defect (i.e. alloying atom). Klemens's expression contains thus three terms:

$$\Gamma = \sum_i \Gamma_i = \sum_i x_i\left\{\left(\frac{\Delta M}{M}\right)^2 + 2\left[\left(\frac{\Delta K}{K}\right) - 2Q\left(\frac{\Delta R}{R}\right)\right]^2\right\} \quad (10)$$

M, K and R are the atomic mass, bulk modulus and bonding length of the matrix and ΔM and ΔK are the difference of each quantity between matrix and introduced compounds. ΔR is the difference of local bonding length caused by a point defect. Q accounts for the accumulative influences on surrounding bonds from the point defect for which Klemens[61] used 4.2 for substitutional impurities and 3.2 for vacancies. Abeles[56] replaced the term $\Delta R/R$ with $\Delta d/R$ where Δd is the difference of bonding length of matrix and alloying atom in their own lattices so that for binary ($A_{1-x}B_x$ type) or pseudo-binary ($(AB)_{1-x}(AC)_x$ type) systems:[20,56]

$$\Gamma = x(1-x)\left[\left(\frac{\Delta M}{M}\right)^2 + \varepsilon\left(\frac{\Delta a}{a}\right)^2\right] \quad (11)$$

ΔM and $\Delta\alpha$ are the difference in mass and lattice constants between two constituents, M and α are the molar mass and lattice

constant of the alloy. The parameter ε is related to the Grüneisen parameter γ and elastic properties.[26,56,58] Abeles wrote ε as:

$$\varepsilon = \frac{2}{9}\left[\left(G + 6.4\gamma\right)\frac{1+r}{1-r}\right]^2 \quad (12)$$

r is the Poisson ratio which for most semiconducting compounds is found[62] between 0.15 and 0.3. G is a ratio between the contrast in bulk modulus ($\Delta K/K$) and that in the local bonding length ($\Delta R/R$). For diamond-like structures $G = 4$ was used by Abeles and the calculated ε leads to consistence between the model and observed thermal conductivities. In general, G is materials dependent and not straightforward to calculate. Thus, while linkage between ε and basic physical properties is revealed by Equation (12) the accurate value of ε should be obtained by fitting experimental results.[26,56] Nonetheless, for simple cubic structures like PbTe and Mg_2Si, ε calculated from Equation (12) using $G = 4$ are within a factor of 3 difference from experimentally determined values.

Due to the great similarity in elastic properties between PbTe and PbSe the constant value of 65 for PbTe suggested in the literature[20] is used in this work for the entire solid solution.

Figure 6 shows the lattice thermal conductivity κ_L at 300 K and 800 K, the electronic thermal conductivity was determined using Lorenz number calculated from the SKB model and assuming acoustic phonon scattering dominant. The calculated Lorenz number has the same degenerate limit of 2.44 but is smaller than that from single parabolic band model as the sample becomes nondegenerate (10% smaller at 300 K when carrier density is on the lower 10^{19} cm^{-3} level). To minimize the influence from uncertainty in resistivity measurement the room temperature κ_L are obtained from lightly doped samples such that the electronic contribution κ_e is very small and the bipolar contribution is also negligible. At 800 K the κ_L of samples with different doping levels are presented and are in reasonable agreement for each composition. The solid solutions show a significant reduction in κ_L at room temperature, at high temperature however such effect is significantly less as is predicted by the theory.

Using 1.9 W/mK and 1.7 W/mK as κ_L for PbTe and PbSe at 300 K and 0.75 W/mK for both at 800 K, the theoretical reduction due to point defect scattering in solid solutions is calculated and plotted in Figure 6, showing good agreement with the experimental results (with Debye temperature taken as 130 K and 160 K for PbTe and PbSe, respectively). The model as well as experimental result indicates a maximum of 45% reduction (relative to that of pure PbTe) in κ_L at room temperature. We notice that previous study on p-type alloys[11] as well as early literature[18] has indicated a larger reduction (maximum 55%) probably due to the different processing or density of defects. At 800 K both experiment and the model indicate a much weaker reduction with a maximum of 20%.

$Si_{1-x}Ge_x$ or $Mg_2Si_{1-x}Sn_x$ are examples where the lattice thermal conductivity in solid solutions is greatly reduced (up to 94% reduction in $Si_{1-x}Ge_x$[13e] and 75% in $Mg_2Si_{1-x}Sn_x$[63]) and hence a significant improvement in zT has resulted. The reduction in $(PbTe)_{1-x}(PbSe)_x$ of 45% (or even 55%) is considerably less than such examples because the mean free path is already small due to efficient Umklapp scattering in lead chalcogenides. In **Table 2** the κ_L reduction is compared among different material systems with the same degree of alloying (30%), together with the magnitude of the contribution from mass ($\Delta M/M$) and strain field ($\Delta\alpha/\alpha$ and ε) contrast. It is seen that the strain field contrast does not change much for different material systems and none of them is large due to the required similarity in lattice constant for the solid solution to form. The PbTe based system has one of the largest ε, which actually leads to the largest total strain contribution among these systems. The mass contrast in $PbTe_{0.7}Se_{0.3}$ on the other hand is small compared to the other systems. The factor with the highest correlation with the thermal conductivity reduction ($\Delta\kappa_L/\kappa_{L,pure}$) is the magnitude of $\kappa_{L,pure}$.

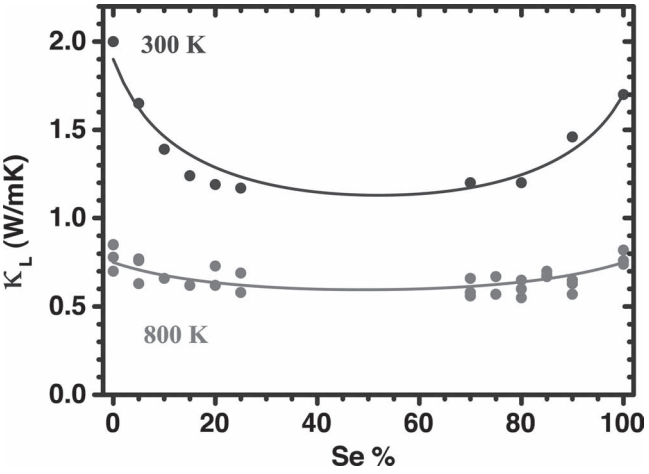

Figure 6. The lattice thermal conductivity at 300 K and 800 K as function of solid solution composition. The solid curve is calculated from the model described in the text.

Table 2. relative lattice thermal conductivity reduction in alloy systems with the same degree of alloying (30%) together with the contribution from mass ($\Delta M/M$) and strain field ($\Delta\alpha/\alpha$ and ε) contrast, ε_{calc} is calculated value from Equation (12).

	$\Delta\kappa_L/\kappa_{L,pure}$ (300 K)	$\Delta M/M$	$\Delta\alpha/\alpha$	ε	ε_{calc}	$\kappa_{L,pure}$ (300 K)	Note
$PbTe_{0.7}Se_{0.3}$	45%	0.15	0.05	65	92	1.9	this work; r = 0.27[a]; γ = 1.45[b]
$Si_{0.7}Ge_{0.3}$	94%[c]	1.1	0.04	39[c]	47	150[c]	r = 0.30[d]; γ = 0.6[e]
$Mg_2Si_{0.7}Sn_{0.3}$	75%[f]	0.87	0.06	23[f]	67	7.9[f]	r = 0.17[g]; γ = 1.3[e]
$Ga_{0.7}In_{0.3}As$	86%[h]	0.29	0.07	45[h]	51	45[h]	r = 0.25[d]; γ = 0.8[e]

Taken from: [a]Ref. [60]; [b]Ref. [34]; [c]Ref. [13e]; [d]Ref. [62]; [e]Ref. [53]; [f]Ref. [63]; [g]Ref. [14d]; [h]Ref. [56].

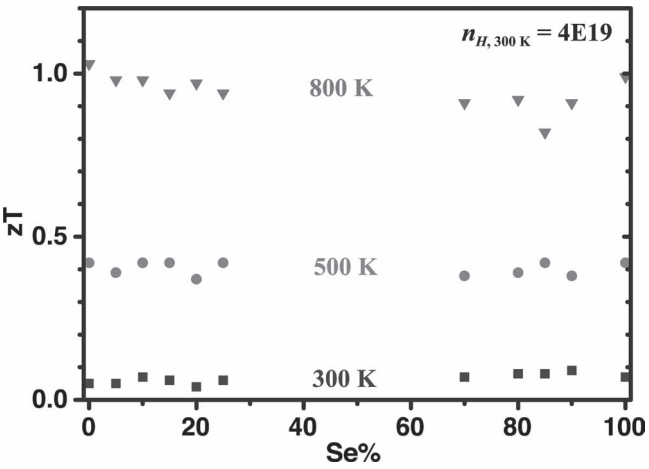

Figure 7. zT at different temperatures for solid solutions with different compositions, doping level is the same for all samples.

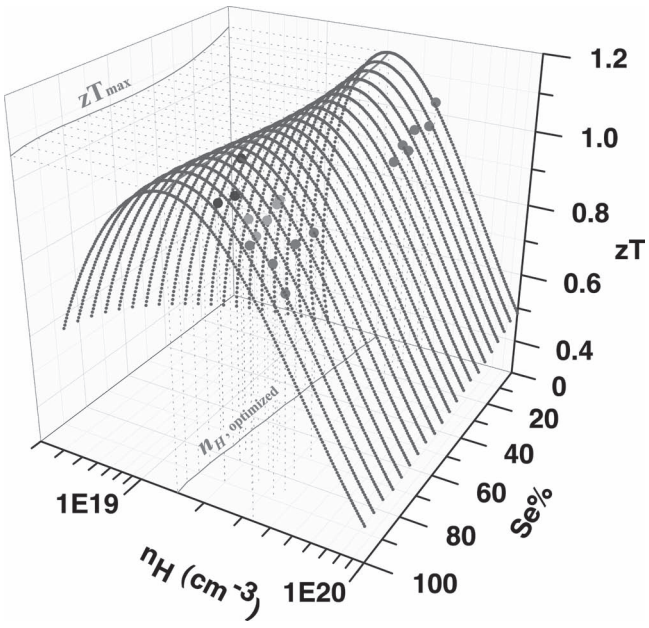

Figure 8. Calculated zT mapping at 800 K for a wide range of alloy composition and Hall carrier density, the maximum zT achievable is almost independent of alloy composition.

2.4. zT Plateau in n-Type $(PbTe)_{1-x}(PbSe)_x$

In the simplest solid solutions, the net result of alloying on zT relies on two effects with opposite influences: mobility reduction and lattice thermal conductivity reduction. In the case of n type $(PbTe)_{1-x}(PbSe)_x$ these two effects are mostly compensated throughout the composition range. In **Figure 7** zT at different temperatures (for samples with $n_{H,300K} = 4 \times 10^{19}$ cm^{-3}) are shown as function of alloy composition and no appreciable difference was observed when Se content change from 0% to 100%.

With all parameters in the transport model determined, zT can be calculated at a given temperature for samples with any carrier density and alloy composition. **Figure 8** shows the zT mapping at 800 K. In addition to the good agreement with experimental data (dots), the maximum zT (solid line) achievable for each composition is found almost unchanged (around 1.1, see the projection on Se%-zT plane). The optimum Hall carrier density is around 2×10^{19} cm^{-3} (see the projection on n_H -Se% plane). A zT plateau is formed where zT is essentially unaffected by the solid solution composition as long as the optimum carrier density is reached, which is not the case for many other systems. The freedom in composition also means that the lattice parameter can be altered in the range of 6.12 Å to 6.46 Å, which may be advantageous for thin film processing or strain engineering.

2.5. The Criteria for Beneficial Disorder in Thermoelectric Solid Solutions

The highest zT that can be achieved in a given material system is governed by its quality factor (Equation (1)). High efficiency thermoelectrics are heavily doped so that the deformation potential (acoustic phonon) scattering is predominant ($\tau_{pure} \approx \tau_{ac}$). In alloy systems incorporating Equation (3) into Equation (5), then substituting Equation (9) for the thermal conductivity one gets:

$$B_{alloy} = T\frac{2k_B^2\hbar}{3\pi}\frac{C_l N_V}{m_I^{*}\Xi^2[1+A(\frac{U}{\Xi})^2]\kappa_{L,pure}arctan(u)/u}, \quad A = \frac{3\pi^2 x(1-x)C_l\Omega}{8k_B T} \tag{13}$$

The relative change of quality factor after forming solid solutions can be written as:

$$\frac{\Delta B}{B_{pure}} = \frac{B_{alloy}}{B_{pure}} - 1 = \frac{u/arctan(u)}{1+\frac{3\pi^2 x(1-x)C_l\Omega}{8k_B T}(\frac{U}{\Xi})^2} - 1 \tag{14}$$

Where u is defined in Equation (9) and Equation (11). Equation (14) being greater than zero indicates a possible improvement of zT in solid solutions. While it is valid over the entire composition range it is more useful to examine the initial effect of alloying, as it will more directly indicate whether the alloying is beneficial or detrimental.

In dilute solid solutions $x << 1$ and $u << 1$, the changing rate of $\Delta B/B_{pure}$ can be expressed as:

$$\frac{d}{dx}\frac{\Delta B}{B_{pure}}\bigg|_{x=0} = \frac{\pi^2\Omega^{1/3}}{k_B T}\left\{\frac{6^{-1/3}\pi^{1/3}\hbar}{k_B\theta_D}\kappa_{L,pure}T\left[\left(\frac{\Delta M}{M}\right)^2+\varepsilon\left(\frac{\Delta\alpha}{\alpha}\right)^2\right]-\frac{3C_l\Omega^{2/3}}{8}\left(\frac{U}{\Xi}\right)^2\right\} \tag{15}$$

The pre-factor $\pi^2\,\Omega^{1/3}/k_BT$, with its $1/T$ dependence, indicates that the disorder in thermoelectrics become less effective

as temperature increases. The main part (inside the braces) contains two terms, which originate from the thermal conductivity reduction and electronic mobility reduction, respectively. The sign of Equation (15) determines whether the solid solution is beneficial (have higher thermoelectric quality factor) compared with the pure compound.

We further note that $\kappa_{L,pure}$ is expected to decrease with temperature as T^{-1} for Umklapp scattering dominant systems, and assuming the other parameters are temperature independent, then the second part of Equation (15) is temperature independent. Thus this part of Equation (15) can all be evaluated from the room temperature materials properties:

$$\left.\frac{d}{dx}\frac{\Delta B}{B_{pure}}\right|_{x=0} = 7.2\times10^{3}\frac{(\Omega^{1/3}/\text{Å})}{(T/K)}\left\{\frac{18.5}{(\theta_D/K)}\times\left(\kappa_{L,pure,300K}/Wm^{-1}K^{-1}\right)\left[\left(\frac{\Delta M}{M}\right)^2+\varepsilon\left(\frac{\Delta\alpha}{\alpha}\right)^2\right]-0.038(C_l/GPa)(\Omega^{2/3}/\text{Å}^2)\left(\frac{U}{\Xi}\right)^2\right\} \quad (16)$$

M and α can be approximated with those for the matrix compound. As the few known values of alloy scattering potential U are around 1 eV (Table 1), this value should be a reasonable estimate for other systems.

Equation (16) provides a criterion determining whether disorder is beneficial for all temperatures from only the values of parameters measured at room temperature. Even though Equation (16) is derived for dilute solid solutions it is qualitatively applicable as a criterion for the full composition range (Equation (14)). Calculations using combinations of realistic material parameters indicate that whenever an appreciable increase of B is achieved for an arbitrary solid solution composition, the rate of $\Delta B/B_{pure}$ in the dilute limit is always large and positive. Thus Equation (16) being greater than zero is a prerequisite of possible zT improvement by forming solid solutions. This criterion is applied to different solid solution systems and the results are listed in **Table 3**.

Equation (16) can be further simplified as $\kappa_{L,pure,300K}$ is related to C_l and θ_D through the speed of sound:

$$C_l = v_l^2 d \quad (17)$$

$$\theta_D = \frac{\hbar}{k_B}\left(\frac{6\pi^2}{\Omega}\right)^{1/3} v \quad (18)$$

where d is the density, v_l is the longitudinal speed of sound, and v is the average speed of sound v given by:

$$\frac{1}{v^3} = \frac{1}{3v_l^3} + \frac{2}{3v_t^3} \quad (19)$$

Since usually the transverse speed of sound v_t is roughly 60% of the longitudinal speed of sound v_l, the ratio v_l/v can be approximated as 1.5 if the exact values are not known. Using the value of 0.096 (a quarter of that used by Toberer et al.[53]) for factor C in Equation (8), reduces Equation (16) to:

$$\left.\frac{d}{dx}\frac{\Delta B}{B_{pure}}\right|_{x=0} = \frac{\pi K\Omega}{4k_B T}\left\{\frac{1}{4\gamma^2}\left[\left(\frac{\Delta M}{M}\right)^2+\varepsilon\left(\frac{\Delta\alpha}{\alpha}\right)^2\right]-10.6\left(\frac{U}{\Xi}\right)^2\right\} \quad (20)$$

the factor C of 0.096 was used in Equation (20) based on the result of study on $(PbTe)_{1-x}(PbSe)_x$ where the two effects of disorder are found almost fully compensated. The examples in Table 3 when evaluated with Equation (20) indicate the same trends in maximum zT change as observed experimentally.

Table 3. the criteria (Equation (16) and Equation (20)), based on the relative change of quality factor, applied to different solid solutions. Only the second part of each equation (inside the braces) is considered. Result is expressed as the thermal conductivity reduction part minus the mobility reduction part. As a comparison the change of maximum zT observed experimentally is also included.

	Equation (16) (κ part–μ part)	Equation (20) (κ part–μ part)	Observed zT improvement
PbTe-PbSe (n)	0.063–0.064	0.025–0.024	not observed, this work
PbSe-PbS (n)	0.016–0.053	0.0075–0.018	$zT\sim1.2$ within uncertainty[a,b]
PbS-CaS (p)	0.16–0.061	0.048–0.015	0.8 to 1.1[c] (900 K), zT for PbS calculated from model
Mg_2Si-Mg_2Sn (n)	0.50–0.10	0.21–0.029	0.7 to 1.1[d,e,f] (800 K)
Si-Ge (n)	9.85–0.22	1.79–0.047	– to 1.0[g] (1100 K)

[a] Ref. [10a]; [b] Ref. [9]; [c] Ref. [60]; [d] Ref. [14a]; [e] Ref. [14b]; [f] Ref. [14c]; [g] Ref. [13f].

Besides the temperature T the effectiveness of disorder for improving thermoelectric performance is affected by several physical properties of the matrix compound. Those with low Grüneisen parameter γ, large deformation potential coefficient Ξ, stiff bonds (large bulk modulus K) and large average volume per atom Ω are more likely to benefit from disorder. Thus for many poor thermoelectric materials that have many of these features, forming a solid solution could potentially enhance their performance greatly. For a given matrix compound, it is best to select a s solid solution component to create as large contrast of mass $\Delta M/M$ and size $\Delta\alpha/\alpha$ as well as a low alloy scattering potential U as possible to achieve the largest improvement of zT by forming solid solution. While these qualitative guidelines are no surprise to the field, Equation (20) gives a quantitative estimate to the improvement in B and therefore zT for each of these effects that can be used to rationally select from a wide range of materials for study.

As a final point we stress that forming a solid solution might also change the band structure (valley degeneracy, effective mass, etc.) as is the case for Si-Ge[64] and Mg_2Si-Mg_2Sn.[65] These effects are not considered here. In experimentally well-examined systems, analysis as outlined above could lead to indications of whether such changes of band structure are present. In systems with theoretical insights on how alloying affects the band structure, Equation (16) and Equation (20) can be used to predict the potential

improvement of zT after adding these influences accordingly as extra terms. Estimates on how the change of band structure affects each parameter in the quality factor B (Equation (1)) would help estimating the sign and magnitude of these terms. In p-type PbTe-PbSe alloy for example, the manipulated band convergence adds a positive term so that a zT improvement is achieved.[11]

In principle, the above analysis, given for isotropic materials, should be applicable to many other classes of thermoelectric materials. However the crystalline anisotropy of many systems (e.g., Bi_2Te_3, Sb_2Te_3, Bi-Sb) makes the measurements and analysis more complicated. For a complete theory the appropriate equations for anisotropic materials would need to be derived including the tensor properties of materials (deformation potential, effective mass, Grüneisen parameter, strain field etc.).

In a broader context, the thermal conductivity reduction due to alloying (through the point defect scattering of phonons) is most effective in scattering high frequency (small wavelength) phonons. Further reduction could be achieved in solid solutions if low frequency (long wavelength) phonons are also scattered by scatterers that produce efficient boundary scattering,[53] such as grain boundaries[66] and larger scale nanostructures.[3] In systems where the electron mean free path is much smaller than this length scale this would result in further zT enhancement.

3. Conclusions

N-type $(PbTe)_{1-x}(PbSe)_x$ solid solutions demonstrate how disorder in solid solutions leads to charge carrier mobility reduction as well as lattice thermal conductivity reduction. These effects can be well explained by transport models based on the atomic and electronic band structures. For n-type $(PbTe)_{1-x}(PbSe)_x$ the reduction in charge carrier mobility almost exactly compensates for the reduction in thermal conductivity leading to no net increase in zT. The verification of this analysis for solid solutions leads to a general criterion that predicts whether a zT improvement is likely when forming certain solid solutions. The criterion suggests that even though materials with low Grüneisen parameter, high deformation potential and stiff bonds are not ideal thermoelectric materials in the pure form, they have the most to gain from disorder in the solid solution form and may ultimately make good thermoelectric materials. It also explains the importance of choosing the constituents based on a large mass and strain contrast while minimizing the alloy scattering potential in order to achieve the largest zT improvement.

4. Experimental Section

In this work we focused on both the Te-rich and Se-rich side of $(PbTe)_{1-x}(PbSe)_x$ solid solution. Br was used as dopant (in form of $PbBr_2$) in Se-rich alloys $(PbTe)_{1-x}$ $(PbSe)_x$ ($0.7 \le x \le 1$) and I (PbI_2) in the counterpart ($0 \le x \le 0.25$). The doping level spans from $n_{H,300\ K} = 1.7 \times 10^{19}$ cm^{-3} to 3.8×10^{19} cm^{-3}. A slight amount of excess Pb is used to minimize metal vacancies[67] as well as improving the mechanical strength.[68]

For each alloy composition, undoped ingots were first made by melting elements at 1373 K (1273 K for Te-rich alloys) for 6 hours. The melted samples were then quenched and annealed at 950 K for 72 hours in the same ampoule. The doped samples were made by adding different amount of dopant ($PbBr_2$ or PbI_2 and Pb) to the undoped chunks and then melting and annealing in the same pattern as undoped ingots. The annealed ingots were ground to powder and sintered at 873 K (823 K for Te-rich alloys) for 60 minutes under 1 atm Ar and 44 MPa pressure using an induction heating hot press.[69] Pellets obtained are ~12 mm in diameter and ~1 mm thick, and are all above 98% of theoretical density.

The in-plane resistivities and Hall coefficients (R_H) were measured using the Van der Pauw method in a magnetic field up to ±2 T. The Seebeck coefficients were measured along the cross-plane direction using Chromel-Nb thermocouples.[70] The thermal conductivities were calculated from $\kappa = dD_TC_p$, with the thermal diffusivity D_T measured along the cross-plane direction by the laser flash method (Netzsch LFA 457) under vacuum with the Cowan model plus pulse correction. The heat capacity C_p was determined using the equation C_p/k_B atom^{-1} = 3.07 + 4.7 × 10^{-4} (T/K-300) by fitting experimental data,[71] which describes C_p for all lead chalcogenides within 2% difference and agrees well with theoretical estimation taking into account[8,72] the Debye heat capacity, the lattice expansion and free carrier contribution. For each measurement data were collected during both heating and cooling and no hysteresis or change in properties were observed. $(PbTe)_{1-x}(PbSe)_x$ system has isotropic crystal structure and in our previous study[9] on PbSe the transport properties were tested both along the in-plane and cross-plane directions and no noticeable difference was observed, which is believed also the case in this study. The uncertainty of each measurement is about 5% which combined could lead to a maximum of 20% uncertainty in zT value.

Acknowledgements

The authors thank Defense Advanced Research Planning Agency's Nano-Structured Materials for Power program and National Aeronautics and Space Administration–Jet Propulsion Laboratory for financial support.

Received: June 12, 2012
Published online: October 22, 2012

[1] L. E. Bell, Science **2008**, *321*, 1457.
[2] a) G. J. Snyder, E. S. Toberer, *Nat. Mater.* **2008**, *7*, 105; b) A. J. Minnich, M. S. Dresselhaus, Z. F. Ren, G. Chen, *Energy Environ. Sci.* **2009**, *2*, 466; c) J. R. Sootsman, D. Y. Chung, M. G. Kanatzidis, *Angew. Chem. Int. Ed.* **2009**, *48*, 8616; d) M. Zebarjadi, K. Esfarjani, M. S. Dresselhaus, Z. F. Ren, G. Chen, *Energy Environ. Sci.* **2012**, *5*, 5147.
[3] M. G. Kanatzidis, *Chem. Mater.* **2010**, *22*, 648.
[4] a) S. N. Girard, J. Q. He, X. Y. Zhou, D. Shoemaker, C. M. Jaworski, C. Uher, V. P. Dravid, J. P. Heremans, M. G. Kanatzidis, *J. Am. Chem. Soc.* **2011**, *133*, 16588; b) Y. Pei, J. Lensch-Falk, E. S. Toberer, D. L. Medlin, G. J. Snyder, *Adv. Funct. Mater.* **2011**, *21*, 241; c) K. Ahn, M. K. Han, J. Q. He, J. Androulakis, S. Ballikaya, C. Uher, V. P. Dravid, M. G. Kanatzidis, *J. Am. Chem. Soc.* **2010**, *132*, 5227; d) Y. Z. Pei, N. A. Heinz, A. LaLonde, G. J. Snyder, *Energy Environ. Sci.* **2011**, *4*, 3640.
[5] a) J. P. Heremans, V. Jovovic, E. S. Toberer, A. Saramat, K. Kurosaki, A. Charoenphakdee, S. Yamanaka, G. J. Snyder, *Science* **2008**, *321*, 554; b) J. P. Heremans, B. Wiendlocha, A. M. Chamoire, *Energy Environ. Sci.* **2012**, *5*, 5510; c) C. M. Jaworski, B. Wiendlocha, V. Jovovic, J. P. Heremans, *Energy Environ. Sci.* **2011**, *4*, 4155.
[6] Y. Pei, A. LaLonde, S. Iwanaga, G. J. Snyder, *Energy Environ. Sci.* **2011**, *4*, 2085.
[7] A. D. LaLonde, Y. Pei, G. J. Snyder, *Energy Environ. Sci.* **2011**, *4*, 2090.

[8] H. Wang, Y. Pei, A. D. Lalonde, G. J. Snyder, *Adv. Mater.* **2011**, *23*, 1366.
[9] H. Wang, Y. Pei, A. D. LaLonde, G. J. Snyder, *Proc. Natl. Acad. Sci.* USA **2012**, *109*, 9705.
[10] a) J. Androulakis, I. Todorov, J. He, D. Y. Chung, V. Dravid, M. Kanatzidis, *J. Am. Chem. Soc.* **2011**, *133*, 10920; b) Q. Zhang, H. Wang, W. Liu, H. Wang, B. Yu, Q. Zhang, Z. Tian, G. Ni, S. Lee, K. Esfarjani, G. Chen, Z. Ren, *Energy Environ. Sci.* **2012**, *5*, 5246.
[11] Y. Pei, X. Shi, A. LaLonde, H. Wang, L. Chen, G. J. Snyder, *Nature* **2011**, *473*, 66.
[12] A. Eucken, G. Kuhn, *Z. Phys. Chem., Stoechiom. Verwandtschaftsl.* **1928**, *134*, 193.
[13] a) M. N. Tripathi, C. M. Bhandari, *J. Phys.-Condes. Matter* **2003**, *15*, 5359; b) G. Joshi, H. Lee, Y. C. Lan, X. W. Wang, G. H. Zhu, D. Z. Wang, R. W. Gould, D. C. Cuff, M. Y. Tang, M. S. Dresselhaus, G. Chen, Z. F. Ren, *Nano Lett.* **2008**, *8*, 4670; c) X. W. Wang, H. Lee, Y. C. Lan, G. H. Zhu, G. Joshi, D. Z. Wang, J. Yang, A. J. Muto, M. Y. Tang, J. Klatsky, S. Song, M. S. Dresselhaus, G. Chen, Z. F. Ren, *Appl. Phys. Lett.* **2008**, *93*, 193121; d) A. J. Minnich, H. Lee, X. W. Wang, G. Joshi, M. S. Dresselhaus, Z. F. Ren, G. Chen, D. Vashaee, *Phys. Rev. B* **2009**, *80*, 155327; e) E. F. Steigmeier, B. Abeles, *Phys. Rev.* **1964**, *136*, A1149; f) C. B. Vining, *J. Appl. Phys.* **1991**, *69*, 331.
[14] a) V. K. Zaitsev, M. I. Fedorov, E. A. Gurieva, I. S. Eremin, P. P. Konstantinov, A. Y. Samunin, M. V. Vedernikov, *Phys. Rev. B* **2006**, *74*, 045207; b) Q. Zhang, J. He, T. J. Zhu, S. N. Zhang, X. B. Zhao, T. M. Tritt, *Appl. Phys. Lett.* **2008**, *93*, 102109; c) S. K. Bux, M. T. Yeung, E. S. Toberer, G. J. Snyder, R. B. Kaner, J. P. Fleurial, *J. Mater. Chem.* **2011**, *21*, 12259; d) R. D. Schmidt, E. D. Case, J. Giles, J. E. Ni, T. P. Hogan, *J. Electron. Mater.* **2012**, *41*, 1210.
[15] a) X. Yan, B. Poudel, Y. Ma, W. S. Liu, G. Joshi, H. Wang, Y. Lan, D. Wang, G. Chen, Z. F. Ren, *Nano Lett.* **2010**, *10*, 3373; b) L. D. Ivanova, L. I. Petrova, Y. V. Granatkina, V. S. Zemskov, *Inorg. Mater.* **2007**, *43*, 933; c) L. N. Luk'yanova, V. A. Kutasov, P. P. Konstantinov, *Phys. Solid State* **2008**, *50*, 2237.
[16] L. S. Stil'bans, DSc Dissertation, A. F. Ioffe Physical-Technical Institute, Leningrad, Leningrad 1960 (In Russian).
[17] a) H. Hohl, A. P. Ramirez, C. Goldmann, G. Ernst, B. Wo lfing, E. Bucher, *J. Phys: Cond. Matter.* **1999**, *11*, 1697; b) C. Uher, J. Yang, S. Hu, D. T. Morelli, G. P. Meisner, *Phys. Rev. B.* **1999**, *59*, 8615; c)C. Yu, T. J. Zhu, R. Z. Shi, Y. Zhang, X. B. Zhao, J. He, *Acta Mater.* **2009**, *57*, 2757.
[18] A. V. Ioffe, A. F. Ioffe, *Sov. Phys.-Solid State* **1960**, *2*, 719.
[19] B. A. Efimova, T. S. Stavitskaya, L. S. Stil'bans, L. M. Sysoeva, *Sov. Phys.-Solid State* **1960**, *1*, 1217.
[20] G. T. Alekseeva, B. A. Efimova, L. M. Ostrovskaya, O. S. Serebryannikova, M. I. Tsypin, *Sov. Phys. Semicond.-USSR* **1971**, *4*, 1122.
[21] A. D. LaLonde, Y. Z. Pei, H. Wang, G. J. Snyder, *Mater. Today* **2011**, *14*, 526.
[22] Y. Pei, A. D. LaLonde, N. A. Heinz, G. J. Snyder, *Adv. Energy Mater.* **2012**, *2*, 670.
[23] Y. Z. Pei, A. D. LaLonde, N. A. Heinz, X. Y. Shi, S. Iwanaga, H. Wang, L. D. Chen, G. J. Snyder, *Adv. Mater.* **2011**, *23*, 5674.
[24] J. Callaway, H. C. Vonbaeyer, *Phys. Rev.* **1960**, *120*, 1149.
[25] P. G. Klemens, *Phys. Rev.* **1960**, *119*, 507.
[26] J. Yang, G. P. Meisner, L. Chen, *Appl. Phys. Lett.* **2004**, *85*, 1140.
[27] a) G. P. Meisner, D. T. Morelli, S. Hu, J. Yang, C. Uher, *Phys. Rev. Lett.* **1998**, *80*, 3551; b) H. Wang, A. Charoenphakdee, K. Kurosaki, S. Yamanaka, G. J. Snyder, *Phys. Rev. B* **2011**, *83*, 024303.
[28] L. Nordheim, *Annalen der Physik* **1931**, *9*, 607.
[29] H. Brooks, in *Advances in Electronics and Electron Physics*, Vol. *7*, Academic Press Inc, NY, **1955**.
[30] F. Herman, M. Glicksman, R. H. Parmenter, in *Progress in semiconductors*, Vol. *2*, John Wiley & Sons, Inc., New York **1957**.
[31] a) R. P. Chasmar, R. Stratton, *J. Electron. Contrl.* **1959**, *7*, 52; b) G. D. Mahan, in *Solid State Physics*, Vol. *51*, Academic Press Inc., San Diego **1998**.
[32] J. Bardeen, W. Shockley, *Phys. Rev.* **1950**, *80*, 72.
[33] P. Lawaetz, *Phys. Rev.* **1968**, *174*, 867.
[34] Y. I. Ravich, B. A. Efimova, I. A. Smirnov, *Semiconducting lead chalcogenides*, Vol. *5*, Plenum Press, New York **1970**.
[35] a) D. J. Singh, *Phys. Rev. B* **2010**, *81*, 195217; b) D. Parker, D. J. Singh, *Phys. Rev. B* **2010**, *82*, 035204.
[36] M. Lach-hab, D. A. Papaconstantopoulos, M. J. Mehl, *J. Phys. Chem. Solids* **2002**, *63*, 833.
[37] Y. I. Ravich, B. A. Efimova, V. I. Tamarchenko, *Phys. Status Solidi B-Basic Res.* **1971**, *43*, 11.
[38] a) Y. I. Ravich, B. A. Efimova, V. I. Tamarchenko, *Phys. Status Solidi B-Basic Res.* **1971**, *43*, 453; b) D. M. Zayachuk, *Semiconductors* **1997**, *31*, 173.
[39] D. I. Bilc, S. D. Mahanti, M. G. Kanatzidis, *Phys. Rev. B* **2006**, *74*, 125202.
[40] Y. Takagiwa, Y. Pei, G. Pomrehn, G. J. Snyder, *Appl. Phys. Lett.* **2012**, *101*, 092102.
[41] Y. I. Ravich, in *Lead Chalcogenides Physics and Applications*, Vol. *18*, Taylor & Francis, New York **2003**.
[42] a) V. A. Saakyan, E. D. Devyatkova, I. A. Smirnov, *Sov. Phys. Solid State USSR* **1966**, *7*, 2541; b) A. N. Veis, V. I. Kaidanov, R. F. Kuteinikov, S. A. Nemov, S. A. Rudenko, Y. I. Ukhanov, *Sov. Phys. Semicond. USSR* **1978**, *12*, 161.
[43] F. E. Faradzhev, *Sov. Phys. Semicond.-USSR* **1984**, *18*, 1311.
[44] W. W. Scanlon, *J. Phys. Chem. Solids* **1959**, *8*, 423.
[45] a)P. F. P. Poudeu, J. D'Angelo, H. J. Kong, A. Downey, J. L. Short, R. Pcionek, T. P. Hogan, C. Uher, M. G. Kanatzidis, *J. Am. Chem. Soc.* **2006**, *128*, 14347; b) J. J. Tietjen, L. R. Weisberg, *Appl. Phys. Lett.* **1965**, *7*, 261.
[46] a) L. Makowski, M. Glicksman, *J. Phys. Chem. Solids* **1973**, *34*, 487; b) V. W. L. Chin, R. J. Egan, T. L. Tansley, *J. Appl. Phys.* **1991**, 69, 3571; c) J. W. Harrison, J. R. Hauser, *Phys. Rev. B* **1976**, *13*, 5347; d) J. R. Hauser, M. A. Littlejohn, T. H. Glisson, *Appl. Phys. Lett.* **1976**, *28*, 458.
[47] Different constants in Equation (2) have been used: the pre-factor used by Makowski and Glicksman is roughly 2 times as large. the one used by Chattopadhyay is 0.5 times as large. Mahrotra used a different pre-factor but the value is very close to that in Equation (2). These reports have been converted using Equation (2) when listed in Table 1.
[48] B. M. Askerov, *Electron Transport Phenomena in Semiconductors*, World Scientific Publishing Co. Pty. Ltd., Singapore, New Jersey, London, Hong Kong **1991**.
[49] L. Y. Morgovskii, Y. I. Ravich, *Sov. Phys. Semicond.-USSR* **1971**, *5*, 860.
[50] a) E. Bellotti, F. Bertazzi, M. Goano, *J. Appl. Phys.* **2007**, *101*, 123706; b) W. L. Li, G. A. Csathy, D. C. Tsui, L. N. Pfeiffer, K. W. West, *Appl. Phys. Lett.* **2003**, *83*, 2832; c) D. Chattopadhyay, *Solid State Commun.* **1994**, *91*, 149; d) V. W. L. Chin, *J. Phys. Chem. Solids* **1991**, *52*, 1193; e) S. R. Mehrotra, A. Paul, G. Klimeck, *Appl. Phys. Lett.* **2011**, *98*, 173503; f) S. H. Wei, A. Zunger, *Phys. Rev. B* **1997**, *55*, 13605.
[51] a) S. Movchan, F. Sizov, V. Tetyorkin, *Semicond. Phys., Quantum Electron. Optoelectron.* **1999**, *2*, 84–87; b) H. Dumont, J. E. Bouree, A. Marbeuf, O. Gorochov, *J. Cryst. Growth* **1993**, *130*, 600.
[52] M. A. Littlejohn, J. R. Hauser, T. H. Glisson, D. K. Ferry, J. W. Harrison, *Solid-State Electron.* **1978**, *21*, 107.
[53] E. S. Toberer, A. Zevalkink, G. J. Snyder, *J. Mater. Chem.* **2011**, *21*, 15843.
[54] a) R. Berman, *Thermal Conduction in Solids*, Oxford University Press, Oxford **1976**; b) H. J. Goldsmid, *The Thermal Properties of Solids*, Dover Publications, Inc., New York **1965**; c) G. Leibfried,

E. Schlömann, *Nach. Akad. Wiss. Göttingen, Math. Phys. Klasse* **1954**, *4*, 71.
[55] a) J. M. An, A. Subedi, D. J. Singh, *Solid State Commun.* **2008**, *148*, 417; b) O. Delaire, J. Ma, K. Marty, A. F. May, M. A. McGuire, M. H. Du, D. J. Singh, A. Podlesnyak, G. Ehlers, M. D. Lumsden, B. C. Sales, *Nat. Mater.* **2011**, *10*, 614.
[56] B. Abeles, *Phys. Rev.* **1963**, *131*, 1906.
[57] E. S. Toberer, A. F. May, B. C. Melot, E. Flage-Larsen, G. J. Snyder, *Dalton Trans.* **2010**, *39*, 1046.
[58] C. L. Wan, W. Pan, Q. Xu, Y. X. Qin, J. D. Wang, Z. X. Qu, M. H. Fang, *Phys. Rev. B* **2006**, *74*, 144109.
[59] L. D. Zhao, J. He, C. I. Wu, T. P. Hogan, X. Zhou, C. Uher, V. P. Dravid, M. G. Kanatzidis, *J. Am. Chem*. Soc. **2012**, *134*, 7902.
[60] J. E. Ni, E. D. Case, K. N. Khabir, R. C. Stewart, C. Wu, T. P. Hogan, E. J. Timm, S. N. Girard, M. G. Kanatzidis, *Mater. Sci. Eng. B*, **2010**, *170*, 58.
[61] P. G. Klemens, *Proc. Phys. Soc. A* **1955**, *68*, 1113.
[62] Electronic Archive on Physical Properties of Semiconductors at Ioffe Physical Technical Institute, available at: http://www.ioffe.ru/SVA/NSM/Semicond/index.html, Accessed: July, 2012.
[63] V. K. Zaitsev, E. N. Tkalenko, E. N. Nikitin, *Soviet Phys. Solid State-USSR* **1969**, *11*, 221.
[64] P. E. Batson, J. F. Morar, *Appl. Phys. Lett.* **1991**, *59*, 3285.
[65] W. Liu, X. Tan, K. Yin, H. Liu, X. Tang, J. Shi, Q. Zhang, C. Uher, *Phys. Rev. Lett.* **2012**, *108*, 166601.
[66] a) D. M. Rowe, V. S. Shukla, N. Savvides, *Nature* **1981**, *290*, 765; b) D. M. Rowe, V. S. Shukla, *J. Appl. Phys.* **1981**, *52*, 7421.
[67] T. L. Kovalchik, I. P. Maslakovets, *Soviet Phys.-Tech. Phys.* **1956**, *1*, 2337.
[68] R. W. Fritts, *Thermoelectric Materials and Devices*, Reinhold Pub. Corp., New York **1960**, 143.
[69] A. D. LaLonde, T. Ikeda, G. J. Snyder, *Rev. Sci. Instrum*. **2011**, *82*, 025104.
[70] S. Iwanaga, E. S. Toberer, A. Lalonde, G. J. Snyder, *Rev. Sci. Instrum.* **2011**, *82*, 063905.
[71] R. Blachnik, R. Igel, *Z. Naturforsch. (B)* **1974**, *B 29*, 625.
[72] O. Delaire, A. F. May, M. A. McGuire, W. D. Porter, M. S. Lucas, M. B. Stone, D. L. Abernathy, V. A. Ravi, S. A. Firdosy, G. J. Snyder, *Phys. Rev. B* **2009**, *80*, 184302.